Three-dimensional electrodes for dye-sensitized solar cells: synthesis of indium–tin-oxide nanowire arrays and ITO/TiO_2 core–shell nanowire arrays by electrophoretic deposition

2009 Nanotechnology 20 055601

(http://iopscience.iop.org/0957-4484/20/5/055601)

Nanotechnology **20** (2009) 055601 (9pp) doi:10.1088/0957-4484/20/5/055601

Three-dimensional electrodes for dye-sensitized solar cells: synthesis of indium–tin-oxide nanowire arrays and ITO/TiO_2 core–shell nanowire arrays by electrophoretic deposition

Hong-Wen Wang[1,5], Chi-Feng Ting[1], Miao-Ken Hung[1], Chwei-Huann Chiou[2], Ying-Ling Liu[3], Zongwen Liu[4], Kyle R Ratinac[4] and Simon P Ringer[4]

[1] Department of Chemistry, Center for Nanotechnology, Chung-Yuan Christian University, Chungli 320, Taiwan, Republic of China
[2] Chemical Engineering Division, Institute of Nuclear Energy Research, No. 1000, Wenhua Road Jiaan Village, Lungtan Township, Taoyuan County 32546, Taiwan, Republic of China
[3] R&D Center for Membrane Technology, Chung-Yuan Christian University, Chungli 320, Taiwan, Republic of China
[4] Australian Key Centre for Microscopy and Microanalysis, Electron Microscope Unit, University of Sydney, Sydney, NSW 2006, Australia

E-mail: hongwen@cycu.edu.tw

Received 27 August 2008, in final form 13 November 2008
Published 12 January 2009
Online at stacks.iop.org/Nano/20/055601

Abstract
Dye-sensitized solar cells (DSSCs) show promise as a cheaper alternative to silicon-based photovoltaics for specialized applications, provided conversion efficiency can be maximized and production costs minimized. This study demonstrates that arrays of nanowires can be formed by wet-chemical methods for use as three-dimensional (3D) electrodes in DSSCs, thereby improving photoelectric conversion efficiency. Two approaches were employed to create the arrays of ITO (indium–tin-oxide) nanowires or arrays of ITO/TiO_2 core–shell nanowires; both methods were based on electrophoretic deposition (EPD) within a polycarbonate template. The 3D electrodes for solar cells were constructed by using a doctor-blade for coating TiO_2 layers onto the ITO or ITO/TiO_2 nanowire arrays. A photoelectric conversion efficiency as high as 4.3% was achieved in the DSSCs made from ITO nanowires; this performance was better than that of ITO/TiO_2 core–shell nanowires or pristine TiO_2 films. Cyclic voltammetry confirmed that the reaction current was significantly enhanced when a 3D ITO-nanowire electrode was used. Better separation of charge carriers and improved charge transport, due to the enlarged interfacial area, are thought to be the major advantages of using 3D nanowire electrodes for the optimization of DSSCs.

1. Introduction

Dye-sensitized solar cells (DSSCs) consist of a porous nanocrystalline titania (TiO_2) film combined with an efficient light-absorbing dye, which allows them to convert light into electricity. Since first presented by O'Regan and Grätzel in 1991 [1], DSSCs have become the subject of active research because they offer reasonable energy-conversion efficiencies, up to 11% to date, at far lower production costs than those of the first-generation silicon-based photovoltaics. Hence, there

[5] Author to whom any correspondence should be addressed.

is strong interest in the future use of DSSCs in specialized applications, especially if their efficiency-to-cost ratio can be further increased.

Production of these oxide solar cells normally involves sintering together a network of TiO_2 nanoparticles to form a film several micrometers thick and establish a pathway for electronic conduction. Subsequently, a monolayer of charge-generating dye is covalently bonded onto the TiO_2 film. Photoexcitation of the dye ejects electrons into the conduction band of the TiO_2 oxide and, if recombination of electrons and holes does not occur within the film, the electrons are subsequently transferred to an electrode and thence to the external circuit. The electrode is typically made from a transparent conducting oxide such as ITO or F-doped tin-oxide (FTO) glass. The original state of the dye is restored by electron donation from the I^-/I_3^- electrolyte reaction, allowing the energy-conversion cycle to begin again [2, 3].

Improvements in the performance of DSSCs depend on optimizing the conduction path and removing the electrons as quickly as possible to avoid recombination of the charge carriers. This can be achieved in several ways. One way is to maximize the area of the dye–oxide interface and improve its conduction. This has been a focus of recent research that has used other types of building blocks, such as one-dimensional (1D) nanowires, to construct DSSCs with enhanced performance through nanoscale effects. ZnO and TiO_2 nanowire-, nanorod- and nanotube-based DSSCs have been reported in which the one-dimensional nanostructures were synthesized by chemical or physical methods [4–11]. Examples have included mixing hydrothermal anatase nanotubes into TiO_2 films [4], growing ZnO nanowires in solution or by MOCVD [5–7], producing TiO_2 nanorods by electrospinning [8] and forming TiO_2 nanotubes by anodic oxidation of titanium plates [9–11]. However, all of the work using these 1D nanostructures focused on the interfacial area of the oxide layer available for the photosensitive dye; the interface between the ITO-glass electrode and the oxide layer was kept flat. Another way to improve cell performance is to maximize the area of this second interface to increase charge capture. To date, however, there have not been any systematic studies of the effect of changes in this interface on cell performance.

A new architecture for DSSCs, focusing on this oxide–electrode interface, was first reported by Cao *et al* [12] and has recently been studied by Joanni *et al* [13]: ITO/TiO_2 core–shell nanowires were synthesized by pulsed-laser deposition to produce a photoelectrode with a high interfacial area. The intention was that the large interfacial area would increase the efficiency of electron transport. Instead, the conversion efficiency of the resulting cells was extremely low (less than 0.15%), due to the thin layer of TiO_2 used in the shells [12, 13]. Nevertheless, we believe that there is genuine merit in the concept of creating a three-dimensional nanostructured electrode to improve DSSC performance, especially if it can be achieved via low-cost wet-chemical processes for the fabrication of oxide nanostructures. In the present study, therefore, we tested this new concept in electrode architecture by synthesizing nanowire arrays with a modified sol–gel approach and evaluating their performance in DSSCs.

2. Experimental procedure

The basic steps of the synthetic process were as follows.

(i) Nanowire arrays were created by EPD of an ITO solution inside the channels of a polymer membrane resting on an ITO-glass substrate (‘method 1’). To make ITO/TiO_2 core–shell nanowires, the insides of the channels were pre-coated with a TiO_2 sol and dried before deposition of the ITO (‘method 2’).
(ii) The polymer-membrane templates were burned off at 500 °C to expose the arrays.
(iii) The arrays were coated with a single layer of an ‘amorphous’ TiO_2 sol, which ensured wetting of the array by subsequent layers of an ‘anatase’ sol that contained suspended TiO_2 nanoparticles. To assess the effect of coating thickness on photoelectric conversion efficiency, two, five or ten layers of the anatase sol were used. Each coating was fired at 450 °C before the next was applied.
(iv) The various coated arrays were made into DSSCs to test their performance.

2.1. Preparation of ITO solutions

The desired ITO stoichiometry was In:Sn = 9:1, a composition known to give good electrical conductivity, and its sol was made as follows [14, 15]. Citric acid monohydrate (99.5%, Showa) was dissolved in a mixture of three parts ethanol and two parts ethylene glycol at 40 °C. The quantity of citric acid was such that its molar amount would be double that of the total molar amount of indium and tin together so that $[C_6H_8O_7{\cdot}H_2O]$:[In] + [Sn] = 2:1. The desired amount of $SnCl_4$ (98%, Alfa Aesar) was added to the citric acid solution and stirred mechanically for 20 min. Then the required amount of $InCl_3$ (99.995%, Acros) was added to the solution and stirred for 2 h. During the final half hour of stirring, sufficient de-ionized water was added to complete the hydrolysis of the precursors at the ratio $[H_2O]$:[In] + [Sn] = 3.1:1, including the water of hydration in the citric acid. At the end of this period, the sol was cooled to room temperature and vacuum filtered with 1 μm filter paper. The final concentration of ITO in the sol was approximately 0.1 M.

2.2. Preparation of the amorphous-TiO_2 sols and the anatase-nanoparticle sols

Two types of TiO_2 sols were prepared: (1) ‘amorphous’ sols [16] and (2) sols containing crystalline anatase nanoparticles [17]. The latter only coats the ITO electrodes if the ITO is first coated with a layer of the former, so the only purpose for using the amorphous sol is to ensure good wetting of the ITO arrays by the anatase-nanoparticle sol. Only a single coating of amorphous sol was used for each sample. Variable numbers of anatase sol (two, five or ten) were applied to different samples to test the effects of TiO_2 thickness on cell performance.

To synthesize the amorphous sol, nitric acid (65%, Riedel-deHaen) was mixed with de-ionized water in a 20 ml glass beaker. Then, titanium butoxide (97%, Sigma-Aldrich) was

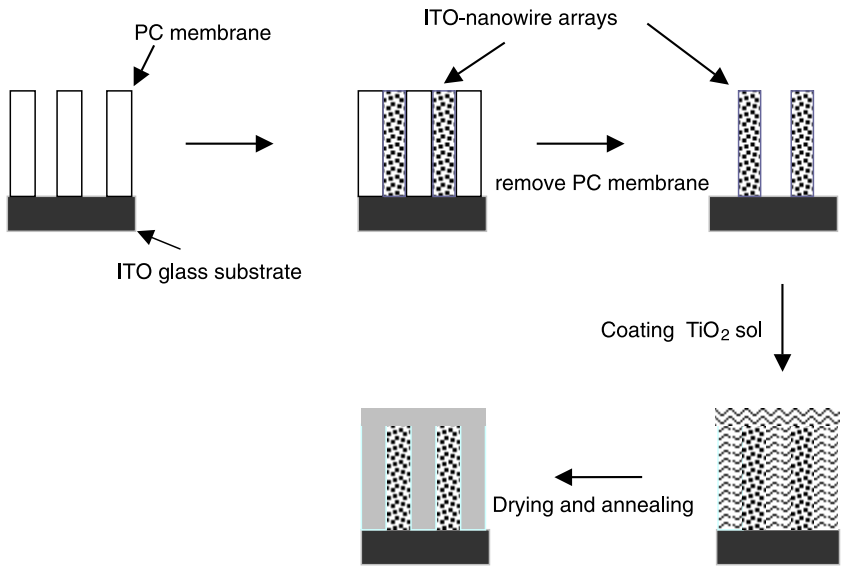

Figure 1. Synthesis of ITO-nanowire arrays and photoelectrode (method 1).

added slowly to the solution. After ageing at room temperature for 1 h, the solution gradually separated into two clear layers. The upper layer was an organic solution and the lower layer was a clear TiO_2 solution. The ratio of Ti:HNO_3:H_2O was 1:1:50. After removal of the top layer by decanting, the TiO_2 sol remained, which we term 'amorphous TiO_2 sol' for clarity.

The anatase nanoparticles were synthesized from a solution of titanium isopropoxide (TTIP, $Ti(OC_3H_7)_4$, 97%, Sigma-Aldrich) subjected to a microwave-heated hydrothermal process as follows. Firstly, a mixture of 37 ml of TTIP and 10 ml of 2-propanol was slowly dripped into a mechanically stirred solution of 80 ml glacial acetic acid and 250 ml de-ionized water at 0 °C [18]. The resulting solution was left unstirred at 0 °C in an ice bath for 4 h. It was then subjected to a microwave-heated hydrothermal process at 150 °C for 3 h in a sealed glass vessel (Discover, CEM Corporation, USA). The resulting suspension contained anatase nanocrystals, which were examined by means of dynamic light scattering (90Plus, Brookhaven Instrument Corporation) and transmission electron microscopy (TEM, JEOL 2010). In the latter case, 50 nanoparticles were measured by manual image analysis to obtain a distribution of particle sizes, which had a mean particle size of 8.9 nm. The mean crystallite size was calculated to be 8.7 nm from the XRD pattern by using Scherrer's equation, which is consistent with that from TEM and the 8.03 nm size obtained from dynamic light scattering.

2.3. Synthesis of ITO or ITO/TiO_2 core–shell nanowire arrays and the TiO_2 coatings

Two methods were used to synthesize the nanowire arrays; both involved forming the arrays within a template by electrophoretic deposition. The first approach, referred to here as 'method 1', produced arrays of ITO nanowires, with nominal diameters of 100 or 200 nm, on ITO-glass substrates. The templates used to make the nanowires were polycarbonate membranes ('PC', Millipore) with parallel and cylindrical pores or channels of 100 and 200 nm in diameter, and a pore density of 10^9 cm^{-2}.

EPD was done with the ITO sol under an electric field of 1.33 V cm^{-1} with a Pt mesh as the counter electrode (anode) and a conducting ITO-glass substrate (ITOCHU Corporation, Japan) as the working electrode (cathode). The cathode was separated from the anode by approximately 2 cm. The templated growth of ITO nanowires was achieved by attaching a PC membrane to the working electrode. Different deposition times allowed the growth of different lengths of ITO nanowires. After the growth was completed, the ITO arrays were dried at 100 °C and then fired at 500 °C for 1 h in air to burn off and remove the PC membrane, leaving the 3D ITO arrays sitting on the ITO-glass substrate. (The surface resistivity of the ITO-glass substrate, which was less than 5 Ω/square, remained stable after heat treatment at 500 °C.) Finally, layers of TiO_2 film were coated on top of the ITO-nanowire arrays by a doctor-blade method in which a layer of amorphous sol was first applied and then two, five or ten layers of anatase sol were applied. Each TiO_2 coating was dried at room temperature for 24 h and then fired at 450 °C for 30 min before the next coating was applied. This layering and firing process produced final TiO_2 layer thicknesses of approximately 7 μm, 12 μm, and 25 μm, respectively (from SEM measurements). Figure 1 illustrates the processing scheme for method 1.

The second process, referred as 'method 2' herein, was employed to synthesize ITO/TiO2 core–shell nanowire arrays on ITO-glass substrates. Figure 2 shows the processing scheme for method 2. The PC membrane was fixed in a special vessel and immersed in an amorphous TiO_2 sol for 1 h, after which the membrane was dried at 50 °C for a few minutes in an oven. In this way, shells of TiO_2 were formed on the inner walls of the membrane's cylindrical pores. Next, ITO cores were formed within the TiO_2 shells by 5 h of templated EPD, under the same

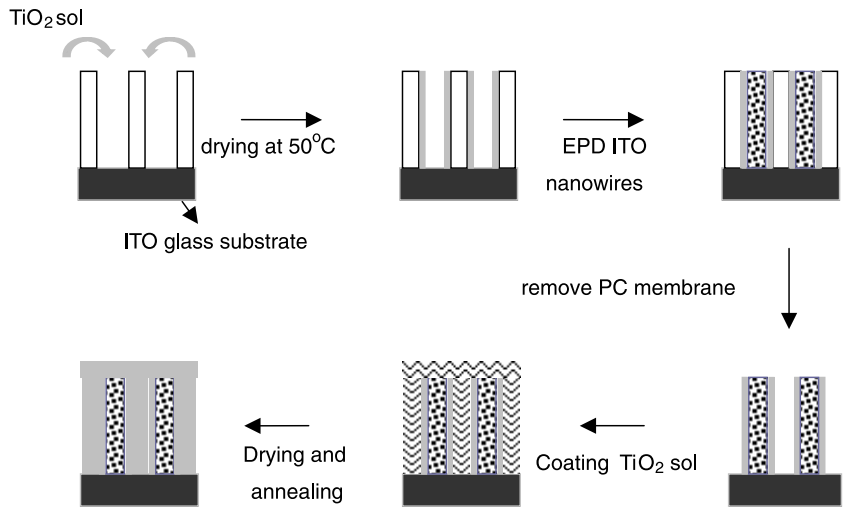

Figure 2. Synthesis of ITO/TiO_2 core–shell nanowire arrays and photoelectrode (method 2).

conditions as described above. The arrays of ITO/TiO_2 core–shell nanowires were dried at 100 °C and then fired at 500 °C for 1 h in air to remove the PC template. Subsequently, the same coating process was applied to the arrays as was used in method 1; one layer of amorphous sol and then two, five or ten layers of anatase sol were applied by doctor-blade. These coatings were dried and fired between each application as described above, again resulting in TiO_2 layers approximately 7 μm, 12 μm, or 25 μm thick, respectively.

2.4. Fabrication of solar cells

After the necessary structural characterization of the specimens (see below), they were fabricated into DSSCs as follows. First, the titania-coated arrays were cleaned with ethanol and then immersed for 4 h in a 5×10^{-3} M solution of the photo-absorption dye Ru(II)$L_2(NCS)_2$, where L is 2,2′-bipyridyl-4,4′-dicarboxylic acid (N3 dye, Solaronix, Switzerland). Samples were also made with the dye [$RuL_2(NCS)_2$]TBA_2, where TBA is tetra-n-butylammonium (N719 dye, Everlight Chemical, Taiwan). After air drying, the dye-coated assemblies were made into solar cells by covering them with an upper Pt-coated glass substrate. Two drops of I^-/I_3^- electrolyte (Iodolyte R-150, Solaronix, Switzerland) were allowed to penetrate each cell by capillary force.

2.5. Characterization

The crystal structures of all specimens were characterized with a Rigaku D/MAX-3C x-ray diffractometer, with Cu Kα radiation and Ni filter, over the angular range of 20°–70° (2θ) at a scanning rate of 4° min^{-1} and a step size of 0.02°. Field-emission scanning electron microscopy (FESEM, Hitachi S-4100) was used to characterize the morphologies of the nanowire arrays and films. TEM characterization was done with a JEOL-2010 fitted with an energy-dispersive x-ray spectroscopy system.

For characterization of the photovoltaic properties, the performance of the solar cells was measured under AM 1.5 sunlight illumination (Model YSS-80, Yamashita Denso, Japan) with a 100 mW cm^{-2} light source. A current/voltage source meter (Model 242, Keithley Instruments Inc., USA) was employed to measure the current and voltage obtained from an illuminated area of 0.4 cm × 0.4 cm. To test the effect of the three-dimensional electrode on the interaction interface, cyclic voltammetry ('CV', CHI 611B electrochemical analyzer, CHI Instruments, USA) was used to compare the performances of three working electrodes: a flat and uncoated stainless-steel disc-type plate (1.3 cm in diameter); a flat stainless-steel disc-type plate coated with an ITO film; and a flat stainless-steel disc-type plate coated with ITO nanowires. The potential scan rate was 0.1 V s^{-1} within the potential range of −0.8–0.6 V. A Pt mesh and an Hg/Hg_2Cl_2 electrode were used as the counter electrode and the reference electrode, respectively. The test solutions were prepared with 0.5 M KOH and 3 M methanol solutions [19]. The ITO film and ITO nanowires for the CV measurements were deposited on the stainless-steel disc-type electrodes by using the same EPD method and conditions used for growing ITO nanowires on the ITO-glass substrates. All photovoltaic properties reported in this work represent the average of data from at least three samples.

3. Results and discussion

Figure 3 shows the XRD patterns of the anatase TiO_2 nanoparticles (synthesized by the microwave hydrothermal method), the TiO_2 nanotubes (from method 2 before the introduction of the ITO), ITO/TiO_2 core–shell nanowires (from method 2) and the ITO-nanowire arrays (from method 1). The broad peaks of these patterns imply that each of these samples contains small crystalline nanoparticles. It is clear from figure 3(a) that crystalline nanoparticles of anatase were readily obtained by using the microwave-heated hydrothermal process at 150 °C for 3 h. TEM micrographs of the titania particles (figure 4(a)) reveal small and approximately equi-axed particles with a narrow size distribution and a mean size of 8.9 nm. The particle size distribution by manual image analysis

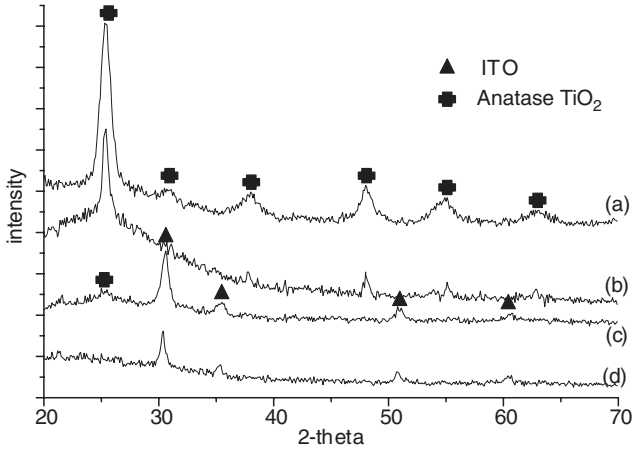

Figure 3. The XRD patterns for (a) anatase TiO_2 nanoparticles synthesized by a microwave hydrothermal process at 150 °C for 3 h (used in both methods), (b) TiO_2 nanotubes fired in air at 500 °C for 1 h (method 2), (c) ITO/TiO_2 core–shell nanowires fired at 500 °C for 1 h (method 2) and (d) ITO-nanowire arrays fired at 500 °C for 1 h (method 1).

is shown in figure 4(a) (lower-left inset). Selected-area electron diffraction (SAED) produced polycrystalline ring patterns consistent with polycrystalline anatase (figure 4(a), upper-right inset). The TiO_2 nanoparticles synthesized by the microwave-heated hydrothermal method exhibit better crystallinity, while requiring significantly less time and energy, than those made by the conventional hydrothermal treatment. The present results agree well with those reported in the literature [18].

The XRD pattern in figure 3(b) confirms that the TiO_2 nanotubes made by method 2 are solely anatase after removal of the PC template by firing at 500 °C for 1 h. After the same template-removal treatment, the crystalline ITO phase is also evident from both methods shown in figures 3(c) and (d), respectively. Pattern (c) contains diffraction peaks from two phases, anatase and ITO, which agrees with the phases expected to be present in the ITO/TiO_2 core–shell nanowires produced by method 2. Figure 4(b) shows a TEM micrograph of a single ITO nanowire, which is polycrystalline (SAED pattern, bottom-left inset), consisting of nanocrystals of ITO particles approximately 10 nm in size (upper-right inset).

The SEM micrographs shown in figure 5 reveal the 3D photoelectrodes at different stages of preparation. Figure 5(a) shows the ITO nanowires after firing at 500 °C for 1 h before coating with the TiO_2 sols (method 1). The nanowires appear to be relatively uniform in diameter and height and reasonably well aligned. There is some deflection of the wires and we suspect this might be due in part to the forces generated during the combustion of the PC template and is not just the inherent shape of the template itself. Given the density of the wires in the array, it also seems likely that there are contacts among the nanowires, which will influence the performance of the electrode. Figure 5(b) shows the ITO nanowires coated with a thin layer of amorphous sol and figure 5(c) shows the sample subsequently coated with five layers of anatase sol (method 1), the surface of which is uniform. As expected, the ITO nanowires were embedded within the bulk TiO_2 films.

Figure 5(d) shows the morphology of the TiO_2 nanotubes that were formed inside the channels of the PC membrane by simple capillary force via method 2. It is evident that several of the nanotubes are joined at their edges, some to such an extent that their pores merge and form single tubes. This is suggestive of a lack of uniformity in the channels in the PC membranes, which obviously are not all entirely isolated from one another. After introduction of the ITO into these nanotubes, we examined the ITO/TiO_2 core–shell nanowires by TEM and a typical micrograph is presented in figure 6(a). The core of the nanowire is quite uniform and

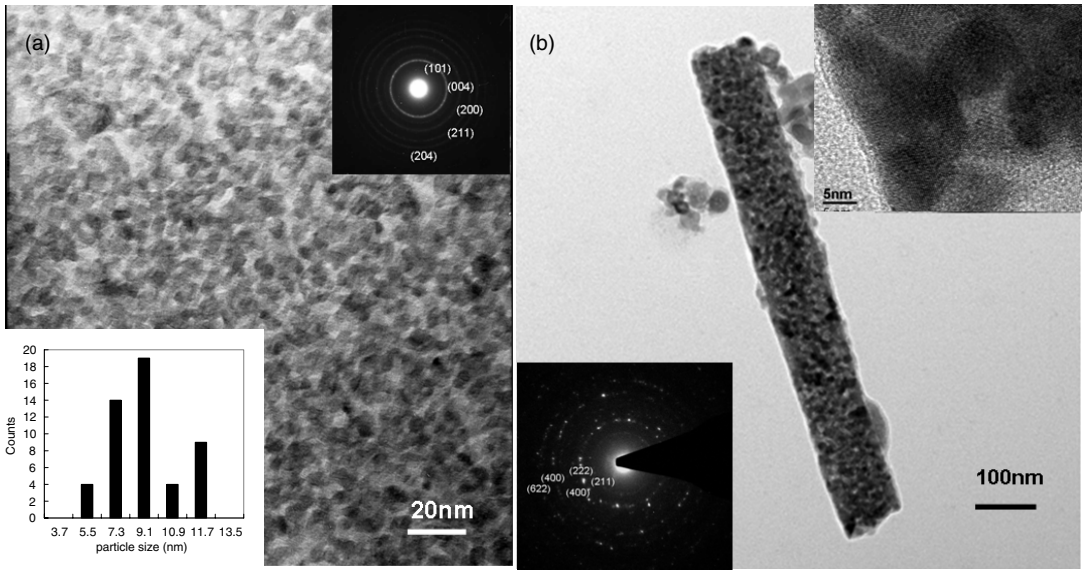

Figure 4. TEM micrographs for (a) anatase TiO_2 nanoparticles size ∼8.9 nm and selected-area electron diffraction (SAED) pattern of anatase TiO_2 nanoparticles, and (b) bright field of a single ITO nanowire, where upper inset is a high-resolution image of the nanowire and lower inset is the SAED pattern of the nanowire. A 100 nm diameter ITO nanowire is shown instead of a 200 nm diameter wire due to its greater electron transparency.

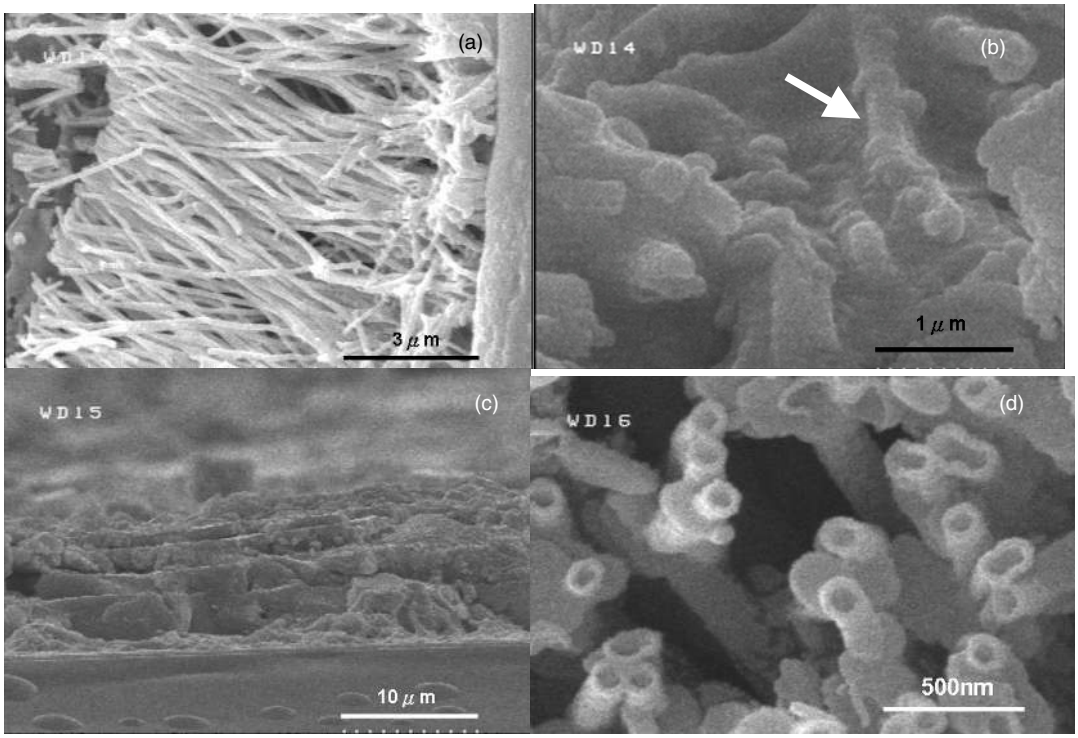

Figure 5. SEM micrographs of (a) ITO nanowires with 100 nm diameter (method 1), (b) ITO nanowires (200 nm in diameter, shown by a white arrow) coated with a layer of amorphous TiO_2 sol (method 1), (c) the sample as shown in (b) after coating with five layers of anatase sol (method 1) and (d) the top view of the TiO_2 nanotubes grown in the 200 nm channels of a PC membrane (method 2).

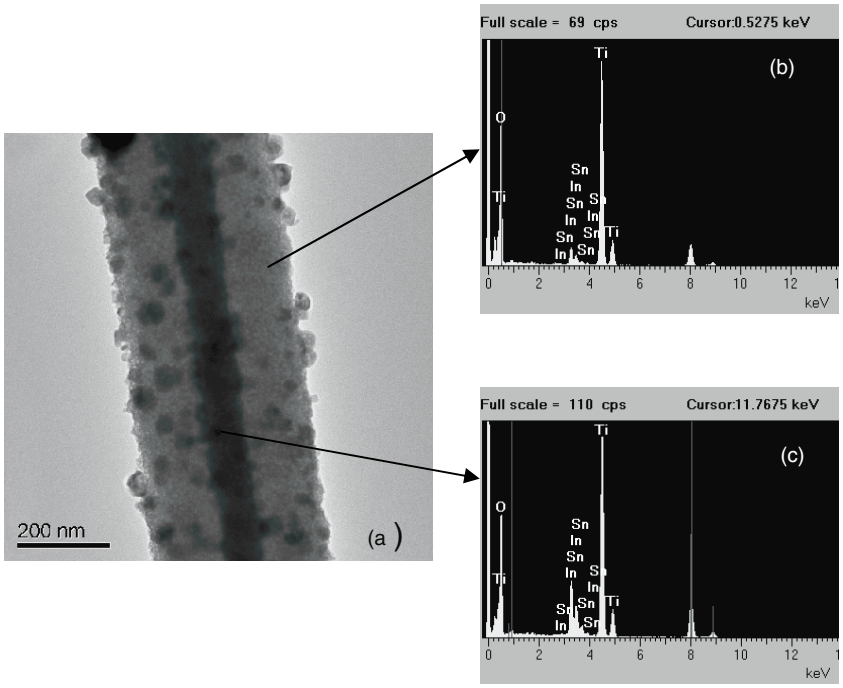

Figure 6. (a) TEM micrograph of a single ITO/TiO_2 core–shell nanowire formed by method 2, (b) and (c) energy-dispersive x-ray spectra of the shell and core–shell, respectively.

shows darker contrast than the shell, as would be expected from the difference in atomic number between the core (In, Sn) and the shell (Ti). The energy-dispersive x-ray spectra shown in figures 6(b) and (c) clearly indicate a greater proportion of In and Sn occur in the core than in the shell, consistent with the characteristic x-rays collected from the ITO core through the TiO_2 shell above and below. It is noteworthy that there are darker spots distributed throughout the TiO_2 shell. These appear, from their contrast and x-ray analysis, to be ITO islands formed during the deposition of ITO solution into the TiO_2

Table 1. Summary of photoelectric conversion efficiencies for a selection of solar cells comparing the performance of flat ITO electrodes with electrodes of ITO nanowire arrays made by method 1.

TiO_2 film thickness (μm)	Nominal nanowire diameter for 3D electrode	Dye	Photoelectric conversion efficiency with flat ITO electrode (%)	Photoelectric conversion efficiency with 3D nanowire arrays (%)	Relative improvement in conversion over 2D electrode
7	200	N3	0.85	1.24	1.46
12	200	N3	3.10	3.99	1.29
12	100	N3	3.10	3.65	1.18
12	200	N719	3.80	4.30	1.13
25	200	N3	1.50	2.10	1.40

nanotubes. In method 2, the TiO_2 nanotubes were only dried prior to the deposition of the ITO solution, which would have penetrated the porous walls of the TiO_2 nanotubes by capillary force. The result is that, after firing, there is a core of ITO and a shell of TiO_2 containing small islands of ITO. A careful TEM examination of samples made by method 2 showed that, while many of the core–shell tubes were like that presented in figure 6(a), some of the nanotubes were only partially filled with ITO and a few remained completely empty. So it is evident that the ITO solution did not always totally fill the TiO_2 nanotubes, probably due to the small inner diameter of the nanotubes. These partially filled and empty tubes will, of course, degrade the photoelectric performance of cells made with the core–shell arrays.

Figure 7 shows the current–voltage (J–V) curves for the samples obtained by irradiating the assembled solar cells with simulated solar light of 100 mW cm^{-2} intensity over an active area of 0.16 cm^2. It is evident that, for samples with the same TiO_2 layer thickness, the ITO-nanowire arrays made by method 1 (samples (a) and (d)) give better performance than the corresponding 2D ITO electrode (samples (b) and (e)) or the corresponding ITO/TiO2 core–shell nanowire arrays made by method 2 (samples (c) and (f)). To further explore these kinds of trends, table 1 summarizes cell performance, as measured by conversion efficiency, for cells made with the 3D ITO-nanowire arrays. As a general point, the use of the ITO nanowire arrays increases the efficiency of all cells above the corresponding cell made with a flat ITO electrode (with relative improvements from 1.13–1.46 times), demonstrating the potential for increasing cell performance by means of using 3D nanostructured electrodes. Considering the effect of the TiO_2 thickness (rows 2, 3 and 6), it is evident that the best absolute efficiency of 3.99% occurs when the TiO_2 layer is 12 μm thick and that this value is substantially higher than that for thinner or thicker oxide layers. Clearly, 12 μm is the optimum of the three thicknesses examined here. It is also clear from table 1 that the use of narrower nanowires (100 nm versus 200 nm; rows 3 and 4) does not improve efficiency. This is consistent with the reduction in the surface area of the oxide–electrode interface (by up to half with all other things being equal) when going from 200 nm diameter wires to 100 nm wires. Finally, it is apparent that using the dye N719 rather than N3 does increase the absolute conversion efficiency somewhat (4.30% versus 3.99%), but that the relative improvement over the flat ITO electrode is reduced. On the basis of these trends, therefore, we will focus on the cells made with 12 μm TiO_2 layers, 200 nm diameter wires and N3 dye.

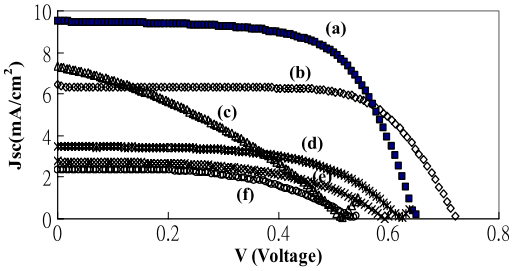

Figure 7. The current (J)–voltage (V) curves obtained by irradiating samples with simulated solar light of 100 mW cm^{-2} intensity over an area of 0.16 cm^2. The samples with a 12 μm TiO_2 film (one layer of amorphous sol and five layers of anatase sol) were (a) ITO arrays (method 1), (b) flat ITO-glass substrate only and (c) ITO/TiO_2 core–shell arrays (method 2). The samples with a 7 μm TiO_2 film (one layer of amorphous sol and two layers of anatase sol) were (d) ITO arrays (method 1), (e) flat ITO-glass substrate only and (f) ITO/TiO_2 core–shell arrays (method 2).

Table 2 summarizes the numerical data from figure 7 for the relevant DSSCs, samples (a), (b) and (c). It is clear that the ITO-nanowire array (sample (a)) exhibits the best performance with a short-circuit current, J_{sc}, of 9.5 mA cm^{-2}, an open-circuit voltage, V_{oc}, of 0.65 V and an overall conversion efficiency, η, of 3.99%. This J_{sc} value is considerably higher than that of the corresponding TiO_2 film (sample (b)) on a flat ITO electrode. This is not due to increased electron mobility, because the latter would not be affected by the difference in area of the oxide–electrode interface. The increase in J_{sc} might be due in part to some increase in the amount of photo-absorption dye attached to the upper surface of the TiO_2 film. The SEM analysis showed greater surface roughness on the micrometer scale for the coated nanowire arrays (e.g. figure 5(c)) compared with the flat ITO electrodes (not shown), and this roughness offered a somewhat larger TiO_2 surface area on which to attach the dye. Nevertheless, we attribute the majority of the improvement in J_{sc} to the substantially increased interfacial surface area between the 3D nanowire electrode and the TiO_2[6]. Thus, when the dye

[6] A theoretical calculation of the increase in interfacial area due to the nanowire arrays illustrates the point. Assume the ideal conditions of 10^9 ITO nanowires, 200 nm in diameter and 10 μm in length (from SEM imaging) per square centimeter of ITO-glass electrode. Also assume that none of the wires contact each other. In this case, the electrode surface area is more than 60 times greater than a flat ITO electrode. Even with an allowance for contact between some of the wires (as is suggested by the SEM imaging of the arrays) by reducing the areal 'density' of nanowires to, say, 1.5×10^8 ITO nanowires per square centimeter of ITO-glass electrode, the available interfacial area is still an order of magnitude larger than that of a flat electrode.

Table 2. Summary of J–V data for solar cells made with N3 dye, in descending order of conversion efficiency, η. For all samples, the TiO_2 layer thickness was 12 μm and the nominal diameter of the nanowires was 200 nm.

Curve in figure 7	Photoelectrode	η (%)	F.F.[a]	J_{sc} (mA cm^{-2})	V_{oc} (V)
(a)	ITO arrays + TiO_2 film (method 1)	3.99[b]	0.63	9.69	0.65
(b)	TiO_2 film	3.1	0.60	7.29	0.72
(c)	ITO/TiO_2 core–shell arrays + TiO_2 film (method 2)	1.3	0.33	7.34	0.54

[a] F.F. = fill factor = maximum output power of cell ÷ ($J_{sc} \times V_{oc}$).
[b] When N719 dye is used, the efficiency goes up to 4.3%, F.F. is 0.53, J_{sc} is 11.94 mA cm^{-2} and V_{oc} is 0.68 V.

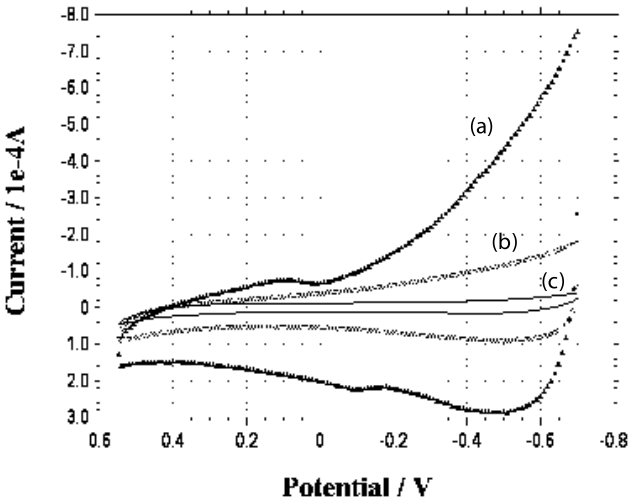

Figure 8. Cyclic voltammetry current–voltage curves for (a) a stainless-steel electrode with ITO nanowires, ▲, (b) a stainless-steel electrode with an ITO film, ○, and (c) a stainless-steel electrode only, −.

is activated and electrons are generated and injected into the conduction band of the TiO_2 layer, the transportation of electrons into the conducting glass substrate, and thence the external circuit, is enhanced by the larger interface of the 3D ITO-nanowire electrode. As more electrons successfully enter the circuit and avoid recombination or recapture, a substantially higher current density is observed at almost all voltages.

It is apparent, too, that the efficiencies of the pristine TiO_2 films (tables 1 and 2) are similar to those in the literature [19], but not particularly high. This is probably because the use of the 8 nm TiO_2 nanoparticles resulted in lower overall performance than larger TiO_2 particles, like P25 (20–30 nm). It is known that particles with larger diameters tend to have better dye adsorption for increased electron–hole generation, resulting in higher short-circuit current density and overall light conversion efficiency [20]. Nevertheless, because we used the same type of anatase sol and the same manufacturing conditions to produce the samples, the effect of the smaller TiO_2 nanoparticles is consistent across all samples.

Table 2 also makes it evident that sample (c), which was made from the ITO/TiO_2 core–shell nanowires by method 2, does not show particularly promising results, with a conversion efficiency of only 1.3%. This is understandable because of the imperfections in some of the ITO cores and the complete absence of cores inside others, as was observed from TEM analysis. Clearly, these imperfections are a technical issue for method 2, emphasizing the importance of ensuring good penetration of the nanotubes by the ITO solution during fabrication. We have begun exploring an alternative synthesis process to solve this problem, the results of which will be reported elsewhere.

To further investigate the benefits of the 3D electrode made from ITO nanowires, cyclic voltammetry (CV) was employed to evaluate the interface activity of three different electrodes: a flat stainless-steel electrode, an electrode coated with an ITO film (1 μm in thickness) and an electrode with an ITO-nanowire array. The three CV curves shown in figure 8 demonstrate the obvious benefits of the 3D electrode made from ITO nanowires. Of the three electrodes, the sample with the nanowire arrays (a) exhibited the largest area within the CV curve; this was 3 times larger than that of the 2D ITO coating and 12 times larger than that of a plain electrode. We attribute this marked improvement to the much larger interfacial area offered by the 3D electrode for electron transfer, resulting in an overall enhancement of its redox activity. The electron pathway between the TiO_2 and the ITO electrode is much improved by using this 3D configuration, leading to the best performance of all the solar cells we examined. Interestingly, these results are much better than those reported previously by Joanni *et al* [13] (0.15% efficiency) or Cao *et al* [12] (0.085% efficiency) for similar geometries. In their work, the TiO_2 film thickness made by sputtering [13] or by sol deposition [12] was too thin (100 nm or 1 μm, respectively) to sustain the electron activities and obviously recombination took place, leading to poor performance. In this study, we embedded the 3D electrodes within an appropriate thickness of TiO_2 film to demonstrate their improved electron transport properties. In all cases, 3D electrodes made by method 1 showed significantly improved performance compared with flat electrodes.

We are seeking further improvement in DSSC performance through refining the synthesis routes, trialing new routes and further optimizing the construction of the cells.

4. Conclusion

We have successfully synthesized arrays of ITO nanowires and ITO/TiO_2 core–shell nanowires by electrophoretic deposition. To ensure the TiO_2 sol thoroughly coated the nanowire arrays, we have developed a two-step coating process: first, applying an amorphous sol and, subsequently, a sol containing anatase nanoparticles. The use of the amorphous sol provided intimate contact with the ITO-nanowire arrays. A 3D electrode made from an ITO-nanowire array embedded within the TiO_2 photoelectrode was constructed with five coatings of anatase sol on top of the amorphous TiO_2 sol (corresponding to a total layer thickness of 12 μm). The photoelectric conversion

efficiency of the DSSCs made in this way reached 3.99% with N3 dye and 4.3% with N719 dye, higher than the efficiencies of a pristine TiO_2 film or arrays of ITO/TiO_2 core–shell nanowires made under the same conditions. Clearly, the use of ITO-nanowire arrays as a 3D electrode for DSSCs is a feasible way to enhance photovoltaic performance, especially with further optimization of the synthesis routes and cell construction.

Acknowledgments

The authors gratefully acknowledge financial support of this research by the NSC-INER project NSC 97-NU-7-033-001, and the Center of Excellence Program on Membrane Technology, the Ministry of Education, Taiwan, ROC. H-W Wang acknowledges the support of the Australian Department of Education, Science and Training (DEST) in the form of an Endeavor Executive Award. The support from the project of the specific research fields in the Chung Yuan Christian University, Taiwan, under grant CYCU-97-CR-CH is also gratefully acknowledged.

References

[1] O'Regan B and Grätzel M 1991 A low-cost, high-efficiency solar cell based on dye-sensitized colloidal TiO_2 films *Nature* **353** 737–40

[2] Grätzel M 2001 Photoelectrochemical cells *Nature* **414** 338–44

[3] Grätzel M 2003 Review dye-sensitized solar cells *J. Photochem. Photobiol.* C **4** 145–53

[4] Wu J J, Chen G R, Lu C C, Wu W T and Chen J S 2008 Performance and electron transport properties of TiO_2 nanocomposite dye-sensitized solar cells *Nanotechnology* **19** 105702–9

[5] Law M, Greene L E, Johnson J C, Saykally R and Yang P D 2005 Nanowire dye-sensitized solar cells *Nat. Mater.* **85** 455–9

[6] Galoppini E, Rochford J, Chen H, Saraf G, Lu Y, Hagfeldt A and Boschloo G 2006 Fast electron transport in metal organic vapor deposition grown dye-sensitized ZnO nanorod solar cells *J. Phys. Chem.* B **110** 16159–61

[7] Baxter J B, Walker A M, van Ommering K and Aydil E S 2006 Synthesis and characterization of ZnO nanowires and their integration into dye sensitized solar cells *Nanotechnology* **17** S304–12

[8] Song M Y, Ahn Y R, Jo S M, Kim D Y and Ahn J P 2005 TiO_2 single-crystalline nanorod electrode for quasi-solid-state dye-sensitized solar cells *Appl. Phys. Lett.* **87** 113113

[9] Wang H, Yip C T, Cheung K Y, Djurišic A B, Xie M H, Leung Y H and Chan W K 2006 Titania-nanotube-array-based photovoltaic cells *Appl. Phys. Lett.* **89** 023508

[10] Zhu K, Neale N R, Miedaner A and Frank A J 2007 Enhanced charge-collection efficiencies and light scattering in dye-sensitized solar cells using oriented TiO_2 nanotubes arrays *Nano Lett.* **7** 69–74

[11] Stergiopoulos T, Ghicov A, Likodimos V, Tsoukleris D S, Kunze J, Schmuki P and Falaras P 2008 Dye-sensitized solar cells based on thick highly ordered TiO_2 nanotubes produced by controlled anodic oxidation in non-aqueous electrolytic media *Nanotechnology* **19** 235602

[12] Chou T P, Limmer S J and Cao G Z 2003 Ordered dye-functionalized TiO_2 nanostructures for photoelectrochemical applications *Nanomaterials and Their Optical Applications*; *Proc. SPIE* **5224** 53–61

[13] Joanni E, Savu R, de Sousa G óes M, Bueno P R, de Freitas J N, Nogueira A F, Longoa E and Varela J A 2007 Dye-sensitized solar cell architecture base on indium–tin oxide nanowires coated with titanium dioxide *Scr. Mater.* **57** 277–80

[14] Limmer S J, Cruz S V and Cao G Z 2004 Films and nanorods of transparent conducting oxide ITO by a citric acid sol route *Appl. Phys.* A **79** 421–4

[15] Alam M J and Cameron D C 2000 Optical and electrical properties of transparent conductive ITO thin films deposited by sol–gel process *Thin Solid Films* **377/378** 455–9

[16] Gopal M, Chan W J M and De Jonghe L C 1997 Room temperature synthesis of crystalline metal oxides *J. Mater. Sci.* **32** 6001–8

[17] Zaban A, Ferrere S, Sprague J and Gregg B A 1997 pH-dependent redox potential induced in a sensitizing dye by adsorption onto TiO_2 *J. Phys. Chem.* B **101** 55–7

[18] Wilson G J, Will G D, Frost R L and Montgomery S A 2002 Efficient microwave hydrothermal preparation of nanocrystalline anatase TiO_2 colloids *J. Mater. Chem.* **12** 1787–91

[19] Lou Y B, Maye M M, Han L, Luo J and Zhong C J 2001 Gold–platinum alloy nanoparticle assembly as catalyst for methanol electrooxidation *Chem. Commun.* 473–4

[20] Chou T P, Zhang Q, Russo B, Fryxell G E and Cao G Z 2007 Titania particle size effect on the overall performance of dye-sensitized solar cells *J. Phys. Chem.* C **111** 6296–302